Cosmic Radiation Exposure on Canadian-Based Commercial Airline Routes

B.J. Lewis, P. Tume, L.G.I. Bennett, M. Pierre and A.R. Green
Royal Military College of Canada, P.O. Box 17000 Stn Forces, Kingston, Ontario, Canada, K7K 7B4

T. Cousins, B.E. Hoffarth, T.A. Jones, J.R. Brisson
Defence Research Establishment Ottawa, Ottawa, Ontario, Canada, K1A 0Z4

Abstract

As a result of the recent recommendations of the ICRP-60 and in anticipation of possible regulation on occupational exposure of commercial aircrew, a two-phase investigation was carried out over a one-year period to determine the total dose equivalent on representative Canadian-based flight routes. In the first phase of the study, dedicated scientific flights on a Northern round-trip route between Ottawa and Resolute Bay provided the opportunity to characterize the complex mixed-radiation field, and to intercompare various instrumentation using both a conventional suite of powered detectors and passive dosimetry. In the second phase, volunteer aircrew carried (passive) neutron bubble detectors during their routine flight duties. From these measurements, the total dose equivalent was derived for a given route with a knowledge of the neutron fraction as determined from the scientific flights and computer code (CARI-LF) calculations.

This study has yielded an extensive database of over 3100 measurements providing the total dose equivalent for 385 different routes. By folding in flight frequency information and the accumulated flight hours, the annual occupational exposures of 26 flight crew have been determined. This study has indicated that most Canadian-based domestic and international aircrew will exceed the proposed annual ICRP-60 public limit of 1 mSv y^{-1} but will be well below the occupational limit of 20 mSv y^{-1}.

1. Introduction

The International Commission on Radiological Protection (ICRP) recently recommended that in-flight natural background exposure of jet aircrew should be considered an occupational exposure.[1] This recommendation resulted from another recommendation to lower the annual stochastic limit for both the general public (from 5 to 1 mSv y^{-1}) and nuclear energy workers (from 50 to 20 mSv y^{-1} averaged over 5 years, with not more than 50 mSv in a single year). In fact, annual jet aircrew dose estimations are expected to be comparable to those recorded for monitored workers in the Canadian National Dose Registry (see, for example, Table 1).[2] At this time, Canadian aircrews are not monitored for natural occupational exposure nor is there a method in place for dose estimation. Furthermore, aircrew exposures from in-flight natural background radiation sources are beyond the mandate of the nuclear regulator in Canada, the Atomic Energy Control Board.[4]

Recently, a number of epidemiological studies on the mortality and cancer incidence for aircrew have been completed, although these studies are somewhat inconclusive.[5-11] For instance, an epidemiological study on Air Canada pilots suggested an increased incidence of prostate cancer and acute myeloid leukemia as compared to the Canadian population.[6] This finding however was not supported in a more recent British Airways study.[7] In addition, Grayson and Lyons argued that population bias was an important issue and considered only flying versus non-flying United States Air Force aircrew for comparative study; i.e., statistically-significant excesses of aircrew cancers were seen for all sites, testis and urinary bladder.[8] Limited investigations have been undertaken for flight attendants as well. The United States National Institute for Occupational Safety and Health (NIOSH), in collaboration with the Federal Aviation Administration, is currently investigating the possible association of health effects as a function of several variables including cosmic radiation and/or disruptions in the circadian rhythm.[9]

Investigations of Finnish female cabin attendants have also indicated elevated risks of breast, leukemia and bone cancer, in comparison to the whole Finnish population.[10,11] However, in all of these studies, the occupational exposure of aircrew has not been precisely determined. For instance, in order to address this shortcoming, the European Commission is currently undertaking an extensive effort to better quantify the cosmic radiation dose through theoretical studies and experimental work including the use of a wide range of detectors on several routes.[12]

In response to such issues, the Air Transport Association of Canada along with selected major, regional and charter air carriers (employers and their unions) agreed to survey Canadian-based aircrew for occupational exposure in which individual members used neutron-sensitive bubble detectors (BDs). This study took place from August 1996 to January 1998, with the principle directive to document the route total (ambient) dose equivalent. Since the neutron BDs are only sensitive to the neutron field, the data had to be scaled to account for all particle types for an estimation of the total dose equivalent. Thus, to better characterise the total cosmogenic field, a suite of conventional instrumentation was also used on dedicated scientific flights. Hence with the extensive survey database and a knowledge of the neutron fraction, these data could then be used by the industry to estimate annual occupational exposure of individual aircrew. With this information, other federal agencies (e.g., Transport Canada) are expected to provide guidelines to the air carriers regarding possible changes, if any, to occupational health and safety practices for aircrew.

Table 1: Average Annual Occupational Exposures*

Category	Occupation	Annual Exposure (mSv)
Mining	Underground uranium miner	10.8
Nuclear Power	Nuclear fuel handler	6.93
Industry and Research	Industrial radiographer	2.75
Medicine	Nuclear medicine technologist	1.08
Airline	Aircrew (pilots and flight attendants)**	~1-5

* Taken from Ref. 3.

** See Section 3.2

2. Experiment

Prior to using the bubble detectors as a standard tool for the survey phase of the study, the detectors were calibrated for in-flight neutron field measurements based upon several particle accelerator studies (Section 2.1). In addition, the detector was better characterized to determine the influence of the cabin environment on the measurement capability of the device (Section 2.2). Finally, the bubble detector was compared to a conventional instrument suite which could measure the distribution and the total dose equivalent (from all particle types) for a given flight route. This latter investigation was supported by a series of scientific flights that provided the means to intercompare several types of passive and active detectors.

2.1 Bubble Detector Calibration

For each route measurement of the neutron dose equivalent (DE_n), the aircrew logged the flight parameters and the number of bubbles (N_B) accumulated over the flight. The (ambient) total dose equivalent (TDE) was subsequently evaluated, after data collection from the aircrew, with the relation:

$$TDE = \frac{DE_n}{f} = \frac{N_B}{f * RD_{amb}} \tag{1}$$

Here f is the neutron fraction as determined from computer calculations with the Federal Aviation Administration (FAA) code CARI-LF.[13] These calculations of the neutron fraction are further supported by the results of the dedicated flights (Section 3.1). The calibration factor for the BD is described by the response-to-(ambient) dose equivalent, RD_{amb}:

$$RD_{amb} = \frac{\int \frac{RF(E)\,\phi(\mathrm{E})}{H*(10)(E)} dE}{\int \phi(\mathrm{E}) dE} = \frac{2.303 \int \frac{RF(E)\,E\,\phi(E)}{H*(10)(E)} d\log(E)}{2.303 \int E\,\phi(E)\,d\log E} \tag{2}$$

where $RF(E)$ is the energy response function of the detector (as determined from high-energy accelerator experiments), $\phi(E)$ is the cosmic-ray neutron flux per unit energy interval at energy E, and $H^*(10)(E)$ is a conversion function of the ambient dose equivalent per unit fluence. The second relation in Eq. (2) is particularly useful when the neutron flux per unit energy is given as a lethargy representation.

For the original calibration, the manufacturer used an AmBe neutron spectrum in combination with a known $RF(E)$ up to 20 MeV and a referenced dose conversion function that predates the current ICRP recommendation. This approach is acceptable for most terrestrial applications where the shape of the spectrum typically extends to approximately 12 MeV.[14] However, for aircrew applications, the calculation of the neutron-dose equivalent (DE_n) must take into consideration the cosmic-ray neutron spectrum. In order to do this, the response function has now been extended to 500 MeV. As shown in Figure 1, the proposed $RF(E)$ is given for a unit detector sensitivity of 1 bubble mrem^{-1} (i.e., 0.1 bubble μSv^{-1}) at a temperature of 20°C. This function is derived from several accelerator studies by Tume et al.[15] and Buckner and Noulty[16] for neutron energies up to 66 MeV, and a theoretical analysis based on the behaviour of the total cross sections for the higher-energy response curve.[15]

To substantiate the proposed response function for the given aircrew application, measurements were also made at the TRI-University Meson Facility (TRIUMF). This facility was chosen since the neutron spectrum generated behind the accelerator shielding provides a reasonable simulation of the neutron spectrum encountered (up to 500 MeV in energy) by aircrew at jet aircraft altitudes (see Figure 2).[15] For instance, the neutron lethargy spectrum measured by Moritz[17] near the beam dump of the 500 MeV proton accelerator at TRIUMF, using a multisphere technique and a $^{12}C(n,2n)^{11}C$ reaction in a plastic scintillator, is similar in shape to the cosmic neutron spectrum (at altitude) as determined recently from both measurement with a multisphere neutron spectrometer (MNS)[18,19] and by Monte Carlo calculations.[20] The various spectra in Fig. 2 have been scaled to the measured spectrum of Goldhagen so that the area under all curves are equal (i.e., the same scalar flux). The derivation of the calibration factor for the bubble detector is not affected by any scaling since the constant scaling factor will cancel in both the numerator and denominator of Eq. (2). The MNS measurements were taken aboard a Canadian Boeing 707 from Trenton, Canada to Koln, Germany on May 9, 1995 at 55°N-58°W at an altitude of 11.3 km (222 g cm^{-2}),[18] and have been corrected for the high-energy charged hadron contribution. The Monte Carlo calculations of Roesler et al. were performed with the FLUKA computer code for 47.4°N-11.0°E at 200 g cm^{-2}.[19,20] The FLUKA calculations are also in good agreement with additional spectral measurements collected on the Zugspite mountain (47.4°N-11.0°E , 2963 m).[20] The thermal component of the two cosmogenic neutron spectra (<1 eV) have been derived from the theoretical analysis of Armstrong et al. based on a Monte Carlo and discrete ordinates method with HETC and ANISN which were scaled accordingly and appended to the latter two curves.[21] Finally, the much older data of Hess et al. are shown for comparison purposes. These data do not contain the 100 MeV feature as observed in all of the other

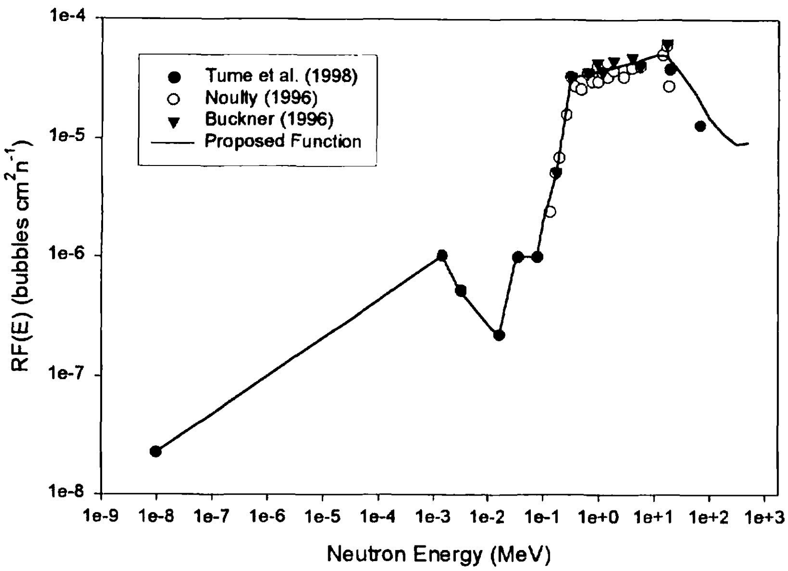

Figure 1. Response-to-fluence function, *RF*(*E*), for a neutron bubble detector with a sensitivity of 0.1 bubble μSv^{-1} (at 20 ^{0}C).

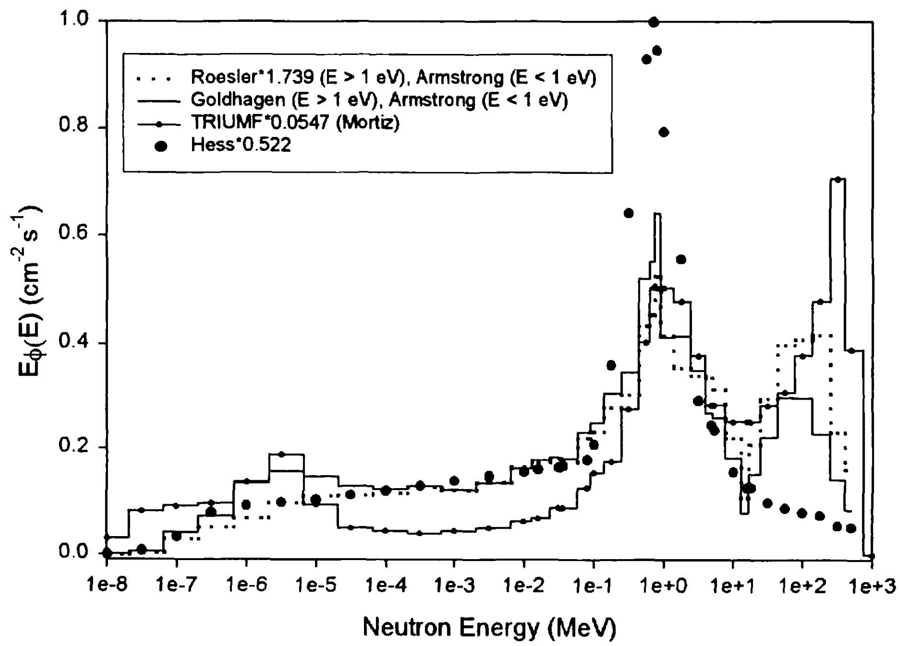

Figure 2. Lethargy plot of cosmic neutron spectra from FLUKA calculations with measurements by Hess et al. and Goldhagen (see text). The simulated cosmic spectrum measured behind the shielding at TRIUMF is also shown.

spectra.[22,23] This result is thought to be due to the antiquity of the measurements as a result of the limited resolution capability of the instrumentation and the unfolding procedure.

The RD_{amb} calculation in Eq. (2) must be referenced to a specified system of dose conversion units. Several modelling reference systems exist for various irradiation conditions and geometry. In this work, the absolute calibration factor for the BD-PND was based on the combined $H^*(10)$ operational units of Siebert et al. (at a 10 mm depth inside an ICRU sphere and below 200 MeV) and Sannikov et al. (at a 10 mm depth on a slab and above 200 MeV) (see Fig. 3).[24,25] In both cases, the authors use a plain, parallel incident neutron beam and ICRP-60 units. Sannikov et al. have argued that this choice of model geometry best represents the equilibrium irradiation conditions for high-energy neutron exposure behind accelerator shielding. By inference, this argument can also be applied to aircrew in which there is atmospheric shielding and a constant source of incident high-energy radiation.

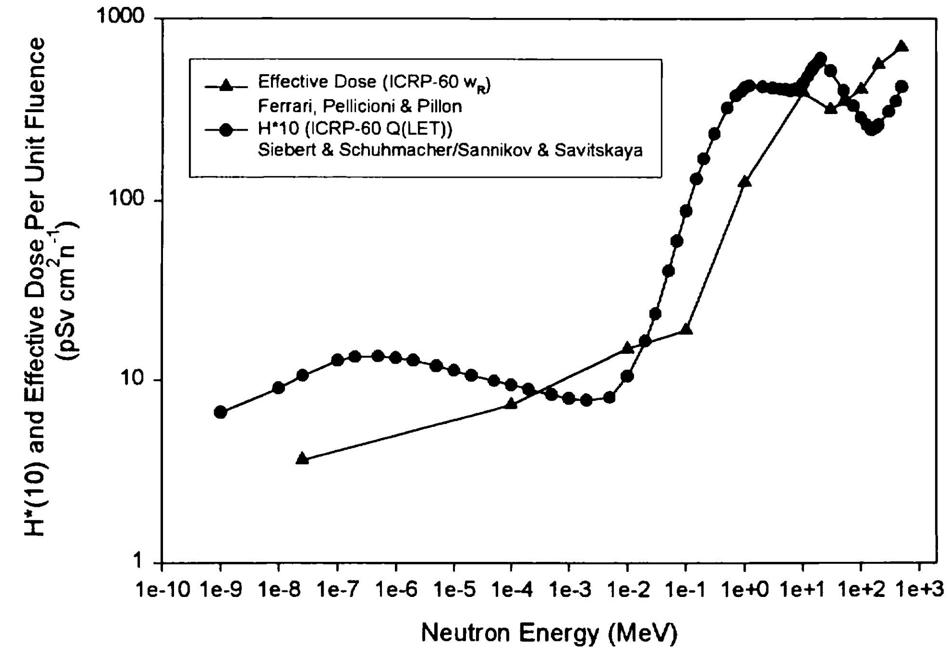

Figure 3. A comparison between the ambient dose equivalent H*(10) and the effective dose per unit fluence.

For a detector with a different sensitivity (other than a unit sensitivity), the curve in Fig. 1 can be suitably scaled. Thus, using Eq. (2) with the respective curves for $RF(E)$ in Fig. 1, the TRIUMF spectrum in Fig. 2, and the stated $H^*(10)$ ambient dose equivalent function in Fig. 3, an integral value of RD_{amb} = 4.0 ± 1 bubble μSv^{-1} is calculated. This calculation is based on a trapezoidal numerical integration rule with a lower integration limit of 1 x10^{-8} MeV and an upper limit of 500 MeV. A 12% temperature correction (i.e., for an ambient temperature of 27°C) has also been applied. This result is for a detector with a given sensitivity of 6 bubble μSv^{-1} as calibrated by the manufacturer in an AmBe neutron spectrum. This integral value is in good agreement with that measured at the TRIUMF Facility (i.e., 5 ± 1 bubble μSv^{-1}). Similarly, the TRIUMF spectrum can be replaced by the measured cosmic neutron spectrum of

Goldhagen (Fig. 2), yielding a final RD_{amb} value of ~4 ± 1 bubble μSv^{-1}. This calculated RD_{amb} value is adopted in the current analysis for Eq. (1). The sensitivity of using different neutron spectra in the calculation is shown in Table 2. Clearly, the feature at 100 MeV (see Fig. 2) does not contribute significantly to the value of RD_{amb}. In addition, the calculated FLUKA spectrum and the measured spectrum of Goldhagen yield equivalent results.

Table 2: Response-to-Dose (*RD*) Conversion Factors*

Spectrum	TRIUMF	Hess	Roesler (FLUKA)**	Goldhagen**
RD_{amb} (bubble μSv^{-1})	3.5	4.3	3.8	3.7
RD_{eff} (bubble μSv^{-1})	7.9	12	8.2	8.7

* Evaluated at 20°C.

** Includes the theoretical spectrum of Armstrong for the thermal neutron contribution.

Fluence-to-effective dose conversion coefficients are now available for various geometrical conditions of irradiation for neutrons from thermal to 10 TeV with the recent FLUKA calculations of Ferrari et al. (see Fig. 3).[26] Thus, the $H^*(10)$ function in Eq. (2) can be replaced by the effective dose per unit fluence function in Fig. 3 (for an isotropic geometry). This calculation yields a response-to-effective dose conversion factor, RD_{eff}, which can be subsequently used in Eq. (1) to replace RD_{amb} in order to provide an effective dose calculation for neutrons. As shown in Table 2, a comparison of these two factors indicates that the operational quantity measured with the neutron bubble detector will provide a conservative estimate (i.e., by about a factor of two) of the effective dose for a cosmogenic neutron-radiation field.

2.2 Bubble Detector Characterisation

Although the BD responds to a range in neutron energies, it is also sensitive to temperature changes and loss of water from inside the detector (i.e., ageing over time). Consequently, the quoted manufacturer's BD sensitivity is valid from 20°C to 40°C, where the manufacturer calibrates the detector at an ambient pressure of 1 atmosphere. These conditions are different from those encountered inside an aircraft where the cabin air is slightly depressurised (equivalent to about 3 km (~10 000 ft)), the humidity is low (~ 5% relative humidity), and the temperature may be as low as 15°C inside some aircraft, particularly during short-haul flights in the Arctic.

An investigation into the effect of air cabin parameters was conducted with a calibrated AmBe source.[27] Pre- and post-calibration tests were carried out to ascertain the degree of BD ageing during the routine operation of the detectors by the aircrew. Tests of the detector sensitivity after the survey period indicated that the drift is generally positive with a magnitude of 15% (i.e., the BDs will record fewer bubbles for the same amount of neutron-dose equivalent).[15] For example, a detector having a pre-calibration sensitivity of 6.0 bubbles μSv^{-1} has a post-calibration sensitivity of 5.1 bubbles μSv^{-1}. However, this trend is within the manufacturer's measured sensitivity of ± 20% for the detectors. During the CARES study, roughly 10% of the 162 detectors exceeded the recommended six-month exchange period.

The major sources of error for the *TDE* estimation in Eq. (1) include the following: the random error for the Poisson counting statistics that corresponds to the square root of the number of bubble observed (~17%);[28] the manufacturer's error due to temperature compensation (20%); the aircrew error in the counting of the number of bubbles (~6%); and the error in the calibration factor RD_{amb} (~25%). Therefore, assuming that these errors are independent, a typical measurement has a ~40% uncertainty.

Having properly characterized and calibrated the BD, this simple (passive) device can be used routinely by aircrew to measure the neutron-dose equivalent. The total dose equivalent then follows by considering the percentage of the neutrons contributing to the total dose equivalent (see Eq. (1)). The neutron fraction can be evaluated by comparing the BD measurement to a suite of conventional instrumentation that is capable of determining the distribution of the total radiation field for all particle types (Section 3.1).

3. Results

3.1 Scientific Flights

A set of scientific flights was conducted on May 6, 1997 aboard a Boeing 727. The 5 flight legs spanned 68 °N to 74 °N latitude from Ottawa, ON (YOW) to Iqaluit (YFB), Iqaluit to Resolute Bay (YRB), Resolute Bay to Nanisivik (YSR), Nanisivik to Iqaluit and Iqaluit to Ottawa. The composition of the mixed radiation field (and hence the neutron fraction) was determined on the scientific flights employing a varied suite of active (i.e., powered) and passive (i.e., non-powered) equipment. This suite consisted of a tissue equivalent proportional counter (TEPC), lead-lined rem-meter (LLRM), ionisation chamber (IC), aluminium oxide thermoluminescent detectors (TLDs) and neutron-sensitive bubble detectors (BDs). Since the TEPC is designed to sample a portion of the charged track left from the passage of the radiation, the measured (lineal) energy spectrum can be approximated by the linear energy transfer (LET) of the particle(s) (see discussion below). This instrument therefore provides a reasonable method to obtain the total absorbed dose and dose equivalent for in-flight measurement. The remaining instruments are sensitive to principally the ionising (i.e., low-LET) or neutron (i.e. high-LET) component of the radiation field.

The output of the TEPC provides the number of counts as a function of the lineal energy (y). This information, in turn, is converted into a probability density function for both the absorbed dose, $d(y)$, and the dose equivalent, $h(y)$ ($= d(y)q(y)$) as derived in the Appendix. The quality factor $q(y)$ can be taken from the International Commission on Radiation Units (ICRU) (publication 40) (i.e., $Q(y)$), or estimated on replacing y by LET and following the standard ICRP-60 recommendation (i.e., $Q(LET)$) (see Fig. 4).[1,29] The spectra are normally represented as $yd(y)$ or $yh(y)$ versus the logarithm of y since, in this representation, equal areas correspond to equal values of absorbed dose or dose equivalent (see Appendix). A summed microdosimetric spectrum for the round-trip scientific flight is shown in Fig. 5.

The dose distribution in the high-LET region has a greater importance when converted to dose equivalent. The relative area under the curve in Fig. 5 below 10 keV/µm indicates that the low-LET contribution is ~13% of the total dose equivalent. The apparent peak in the $yh(y)$ curve near 140 keV/µm is called the "proton edge" and represents the maximum energy that can be deposited by a recoil proton.[30] Although some scatter in the data is evident above 700 keV/µm, this region represents only a small fraction (~ 2%) of the total dose equivalent; however, these data are real and represent the production of high-LET particles due to fragmentation of atmospheric nuclei with high-energy protons. The scatter is principally due to statistics associated with fewer counts in the high lineal-energy bins. Similar spectra for commercial aircraft routes have been obtained by Schuhmacher and Schrewe.[34]

Because of the uncertainty in the direct relationship between LET and y, the data were processed using both of the recommendations in Fig. 4. As shown in Fig. 6, the integrated area did not significantly vary between the two representations, i.e., the dose equivalent was only 7% higher with the $Q(y)$ relationship. Consequently, the TEPC dose equivalent as derived from the standard ICRP-60 $Q(LET)$ recommendation is acceptable for radiation protection purposes and has been adopted for the present analysis.

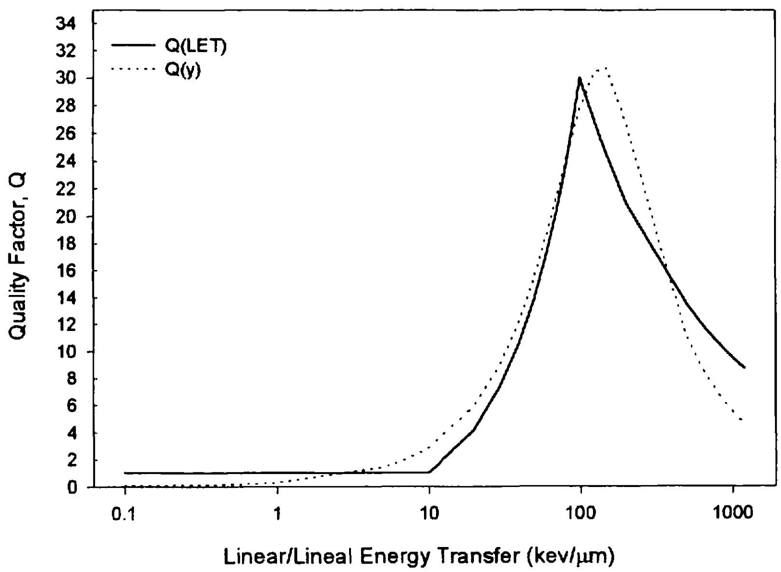

Figure 4. Quality factor as a function of linear energy transfer (*LET*) and lineal energy (*y*).

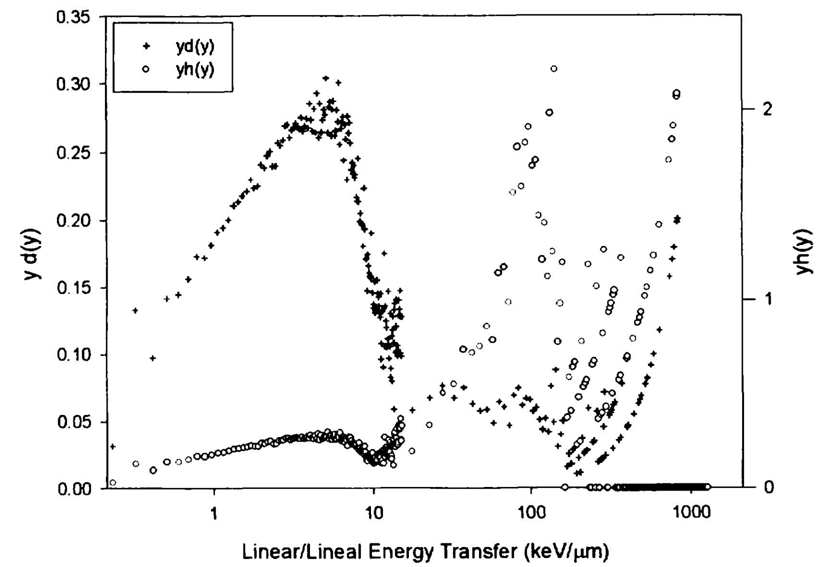

Figure 5. Absorbed dose, *yd*(*y*) as a function of lineal energy, *y*, for the round-trip scientific flight. The dose equivalent distribution, *yh*(*y*) was derived using the *Q*(*LET*) relationship (for an ICRP-60 recommendation) as shown in Fig. 4.

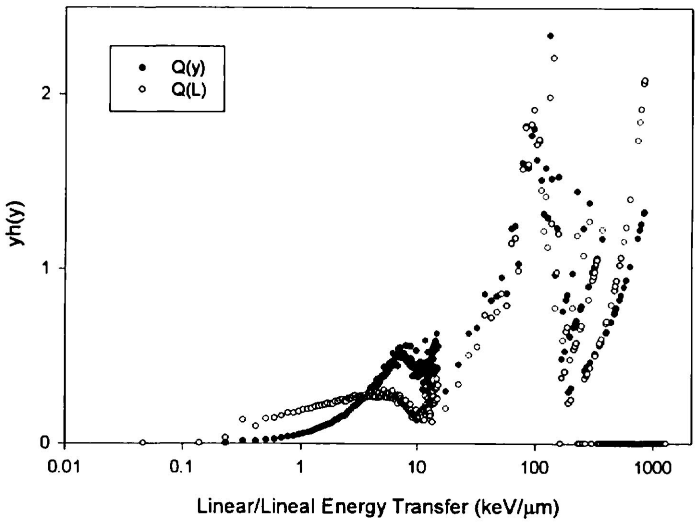

Figure 6. Calculation of the dose equivalent distribution for ICRP-60 and ICRU-40 recommendations.

The total dose equivalents (with absolute error) as measured by the various instruments on the scientific flights are given in Table 3. As shown, the low-*LET* measurements from the (active) IC are in good agreement with the (passive) TLD results. A similar observation was made for the high-*LET* measurement with the (active) LLRM and the (passive) BDs (BD-Flight). Furthermore, the BD measurements from the scientific flights (BD-Flight) are in agreement with those obtained during the survey part of the study (BD-Database) (Section 3.2). In addition, the TEPC results are in agreement, to within experimental uncertainty, with the sum of the low-*LET* and high-*LET* measurements for the various combinations of passive and active instruments. These results indicate that: (i) the low-*LET* and high-*LET* components can be measured with either choice of active or passive detectors; (ii) the bubble detector is sensitive to about half of the in-flight total dose equivalent; and (iii) at high latitudes, the percentage of the low-*LET* and high-*LET* components to the total dose equivalent are relatively constant for northern flights because of the presence of the geomagnetic knee at 57 °N.

The slight discrepancies between the BD-Flight and BD-Database measurements in Table 3 may be explained by the random uncertainties discussed in Section 2.2, and the day-to-day changes in altitude profile for a given route.

As shown in Table 3, the effective dose estimates that are calculated for the scientific flights with the CARI-LF code are slightly underpredicted as compared to the measured ambient dose. It is worthwhile to note that while both the TEPC and CARI-LF use ICRP-60 units, the Quality Factor (Q) versus LET relationship used by the TEPC for operational units should conservatively estimate the protection quantities defined by the weighting factors used in CARI-LF. This statement is also reflected in the calculation of the conversion factor *RD* in Section 2.1 (see Table 2) where the operational quantity measured with the neutron bubble detector will provide a conservative estimate of the effective neutron dose.

Table 3: **Comparison of CARI-LF Effective Dose and Measured Ambient Dose Equivalents From Various Instruments For Flight Legs Between Ottawa, ON to Resolute Bay, NWT on May 6, 1997**

Location Pair	Predicted CARI-LF Effective Dose (μSv)	Measured Ambient Dose Equivalent (μSv)						
		Total Dose Equivalent	Ionising Field (low-LET)		Neutron Field (high-LET)		
		TEPC	Ionization Chamber	TLDs Passenger	BD Flight	BD Database	LLRM
YOW-YFB	10	14 ± 7	3.4 ± 0.4	N/A	5± 2	6± 2	10± 2
YFB-YRB	6	11 ± 5	2.4 ± 0.02	N/A	5± 2	5± 2	5.4± 1
YRB-YSR	0.8	2 ± 1	0.3 ± 0.03	N/A	3± 1	1± 1	0.6± 0.1
YSR-YFB	6	9 ± 3	2.2 ± 0.02	N/A	5± 2	3± 2	4.8± 1
YFB-YOW	13	18 ± 12	4.4 ± 0.04	N/A	11± 4	7± 2	10.2± 2
TOTAL	*36*	*54 ± 28*	*13 ± 0.5*	*15± 2*	*29± 11*	*22± 7*	*31± 6*

The neutron fractions for the scientific flights are calculated in Table 4 by taking the ratio of the ambient dose equivalent from the bubble detector to the total ambient dose equivalent as measured for all particles with the TEPC in Table 3. The flight data between YRB-YSR were not considered in this analysis due to the poor counting statistics resulting from the short flight duration and low altitude profile. As previously discussed, BD-Flight is derived from data collected during the scientific flights while BD-Database are the averaged data from the survey database for the given flight route (see Section 3.2). The measured neutron fractions (i.e., 0.40 – 0.60) are in good agreement with the round-trip average estimate provided by CARI-LF which is based on the ratio of the corresponding effective doses (i.e., 0.51).

Table 4: **Intercomparison of Neutron Fractions From Scientific Flights And Survey Measurements Versus CARI-LF**

Location-Pair	Neutron Fraction, f		
	Measured		Predicted[a]
	BD-Flight / TEPC	BD-Database / TEPC	CARI-LF
YOW-YFB	0.36 ± 0.23	0.43 ± 0.26	0.51
YFB-YRB	0.45 ± 0.24	0.45 ± 0.24	0.51
YSR-YFB	0.56 ± 0.28	0.33 ± 0.25	0.51
YFB-YOW	0.61 ± 0.50	0.39 ± 0.29	0.50
Average[b]	0.50 ± 0.31	0.40 ± 0.26	0.51

a: Based on effective dose calculations.
b: These values exclude the flight from YRB to YSR.

Because not all of the surveyed routes in Section 3.2 could be flown with the powered equipment suite, only the routes of Table 3 are available to date. However, these flights demonstrated that the neutron fractions obtained experimentally (Table 4) were in good agreement with those predicted by CARI-LF. Hence, the neutron fractions, f, as obtained from CARI-LF are used entirely for the calculation of the route *TDE* in Eq. (1).

3.2 Survey Results

Using the methodology of Section 2, the route total dose equivalent was calculated with Eq. (1) for the observed number of bubbles on a given route. The Canadian Aircrew Radiation Environment Study (CARES) Database Management System (CDMS) was developed to handle these survey data consisting of over 3100 individual measurements on 385 different routes.[35] The CDMS was developed using the commercial software package Microsoft® Access 97. This software package was designed to handle both dosimetry data input/output and the on-line extraction of both route and individual cumulative total (ambient) dose equivalent (CTDE).

Table 5 shows the ambient dose equivalents for several representative flight routes from the survey database and compares these with CARI-LF effective dose calculations. The results in Table 5 show that, within experimental error, the CARI-LF predictions are in good agreement with the measured route total (ambient) dose equivalent (RTDE) data obtained during the survey. The trend between the measured and predicted results is more clearly illustrated in Fig. 7, which shows a comparison plot for 250 routes where flight history information was available in the database. The dark solid line with a slope of unity in the figure represents perfect agreement. As seen in Fig. 7, at route doses lower than 20 μSv (i.e. for about 75% of the routes surveyed), the measured RTDE values appear to agree with those predicted by the CARI-LF software. At higher dose levels (usually longer international routes), the measured RTDE values are generally lower than the corresponding predicted route effective doses from CARI-LF as shown by the thin solid line (best fit line of all 250 points).

Table 5: Route-Specific Ambient Dose Equivalent Measurements Versus Predictions using CARI-LF with the Associated Neutron Fractions

			Route Dose (μSv per flight)		Neutron Fraction,[a] f
Grouped Global Flight Region	Sample Route	Scheduled Flight Time	Measured Ambient Dose Equivalent	CARI-LF Effective Dose	CARI-LF
Trans-Pacific	PEK-CYVR	10h 40min	46±10	47	0.47
Trans-Atlantic	CYVR-LHR	9h 6min	40±17	43	0.50
Trans-Canada	CYYZ-CYVR	4h 26min	22±6	25	0.49
Caribbean	CUN-CYYZ	3h 37min	22±4	14	0.46
Northwest/Yukon Territories	CYOW-CYFB	2h 50min	11±4	10	0.51
Pacific	MNL-HKG	1h 43min	3±2	3.4	0.34

a. Based on effective dose calculation.

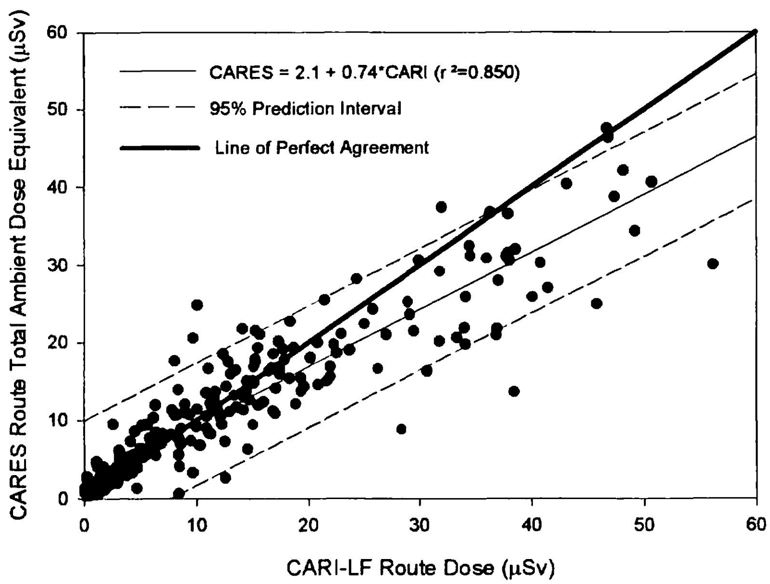

Figure 7. Comparison of the measured route total (ambient) dose equivalent with the CARI-LF effective dose predictions for the same altitude history and route.

Of the 98 persons participating in the survey, only 18 aircrew reported a cumulative (ambient) total dose equivalent (CTDE) in excess of 1 mSv. (These 18 aircrew had an average CTDE of 1.6 ± 0.6 mSv and a mean recorded flight time of 425 ± 137 h for the sample year). However, this result is not necessarily indicative of their actual annual (ambient) total dose equivalent (ATDE), since the detectors were not always used by the individuals during all of their routine duties. In order to estimate the annual exposure actually experienced by the aircrew, the CTDE was scaled for those individuals where the actual employee flight records were available (assuming a similar flight schedule throughout the year) (see Table 6). In this case, five airlines provided the employee flight hours for 26 aircrew (divided into groups of flight attendants (FA), pilots (P), and those aircrew for which no specific occupation was listed (AC)). These data are also displayed in Fig. 8 which shows that roughly 95% of the ATDE estimates for these aircrew exceeded the 1 mSv y^{-1} proposed ICRP-60 public effective dose limit, although all aircrew were below the 5 mSv y^{-1} current public limit. For the given sample, the ATDE received by the flight attendants was greater than that for the pilots on average due to the longer occupational exposure time as a result of a greater number of flights in the year. Furthermore, FA-A who was pregnant during a portion of the survey, was below the proposed ICRP limit of 2 mSv y^{-1} for pregnant workers, but exceeded the proposed annual limit of 1 mSv y^{-1} for the public. These values are also below the potential action limit of 6 mSv y^{-1} proposed by the United Kingdom in response to the European Basic Safety Standards Directive.[36,37]

4. Summary

In summary, the Canadian Aircrew Radiation Environment Study has provided the largest database of route-specific ambient dose equivalent measurements for Canadian-based domestic and international routes. From these measurements, a methodology was developed to evaluate annual ambient dose equivalent estimates for individual pilots and flight attendants. From this analysis, the current data indicate that most Canadian-based domestic and international aircrew will exceed the 1 mSv y^{-1} recommended annual ICRP public limit. However, if aircrew are considered occupationally exposed workers, then they are well below the proposed ICRP limit of 20 mSv y^{-1}. Consequently, these measurements provide an important first-step in establishing the guidance and regulation policy for Canadian-based aircrew occupational exposure.

Table 6: Individual Total Dose Equivalent For A Subset of Survey Participants

ID	Coverage	Aircraft	CTDE (mSv)	Individual Flight Hours, Z	Employer Flight Hours, Y	ATDE[a] (mSv)
FA-A	North, Domestic	B-727	0.19	59.4	366	1.17
FA-B	North	B-727	0.16	50.4	769	2.44
FA-C	North, Domestic	B-727	1.4	311	954	4.29
FA-D	Intl./Domestic	A-320,B-757,EA-32	0.68	194	1042	3.65
FA-E	Intl./Domestic	A-320,B-757	1.5	362	1133	4.69
FA-F	Intl./Domestic	A-320,B-757	1.1	327	1187	3.99
FA-G	Intl./Domestic	A-320,B-757	1.3	409	1107	3.52
FA-H	Domestic	DC-9	0.07	43.1	774	1.26
FA-I	Intl.	A-340,B-747,B-767	0.82	250	835	2.74
FA-J	Intl.	B-747,B-767	1.0	171	797	4.66
FA-K	Domestic	B-747,B767	0.43	90.5	898	4.27
FA-L	Domestic	A-320,B-727,DC-9	0.36	128	713	2.01
FA-M	Intl./Domestic	A-320,B-747,B-767	0.44	109	669	2.70
FA-N	Intl./Domestic	B-767	2.5	572	720	3.15
FA-O	Intl./Domestic	DC-10,B-727, B-737,B-747,B-767	1.3	502	889	2.30
P-A	North, Domestic	B-727	1.6	415	635	2.45
P-B	Domestic	F-28	0.13	52.1	295	0.74
P-C	Domestic	F-28	0.23	105	457	1.00
P-D	Domestic	F-28	0.44	153	549	1.58
P-E	Domestic	F-28	0.40	182	444	0.98
P-F	Intl./Domestic	B-757	1.3	317	852	3.49
P-G	Intl./Domestic	A-320,EA-32	0.52	133	864	3.38
AC-A	Intl.	B-767	1.3	305	684	2.92
AC-B	Intl./Domestic	DC-10,B-747,B-767	2.2	619	911	3.24
AC-C	Intl./Domestic	DC-10,B-767	2.1	665	853	2.69
AC-D	Intl./Domestic	B-767	2.4	473	763	3.87

a: Annual (Ambient) Total Dose Equivalent (ATDE) = CTDE x (Y/Z)

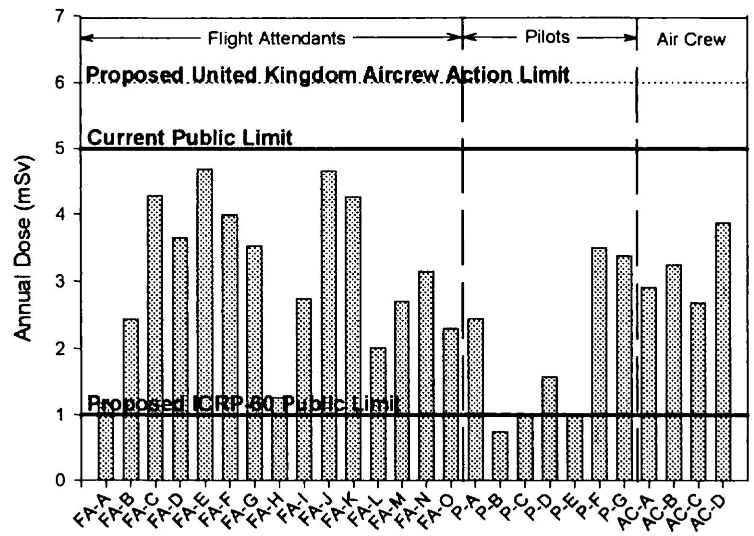

Figure 8. Distribution of aircrew grouped by annual dose equivalent.

Acknowledgements

The authors would like to thank H. Goldberg of the Air Transport Association of Canada (ATAC) and C. Thorp of the Director General Nuclear Safety (DGNS) of the Department of National Defence for their assistance in the study. The authors would also like to express their gratitude to J. Lafrance and the management of First Air for arranging the scientific flights. The co-operation of the management, employees and their unions of Air Canada, Canada 3000, Canadian International, Canadian Regional and First Air in carrying out this survey is greatly appreciated. Our on-going appreciation is extended to the technical personnel of TRIUMF. Finally, the authors would like to thank P. Goldhagen of the Environmental Measurements Laboratory for providing the cosmic neutron spectrum, and W. Friedberg of the Federal Aviation Administration and K. O'Brien of Northern Arizona University for the CARI-LF code.

This study was financially supported by ATAC and DGNS.

Appendix: Microdosimetry Theory

Energy deposition in the TEPC ionizes the detection gas and produces an electronic signal that is collected at the detector anode. A multichannel analyzer (MCA), which measures the pulse size received by the counter, processes the signal. The pulse heights are assigned to a lineal energy bin from which an event frequency distribution may be obtained. Processing of the TEPC data is a non-trivial process, which is briefly explained below to aid in the data interpretation of Section 3.1.[30-33]

The lineal energy, y, is the quotient of the quantity of energy imparted to matter in a volume of interest (by the passage of radiation) to the mean chord length in the volume (see the following derivation). From probability theory, the probability that the lineal energy is equal to or less than y is given by the cumulative distribution function $F(y)$:[33]

$$F(y_i) = \frac{\sum_{i=0}^{i} n(y_i)}{\sum_{i=0}^{\infty} n(y_i)} \tag{3}$$

where $n(y_i)$ is the number of counts registered by the TEPC in a given lineal energy channel i. The probability density (or lineal energy distribution) is further defined from probability theory as:[33]

$$f(y) = \frac{dF(y)}{dy} \approx \frac{\Delta F(y_i)}{\Delta y_i} \equiv f(y_i), \tag{4}$$

and normalized such that:

$$\int_0^{\infty} f(y)dy = 1. \tag{5}$$

For the numerical implementation of Eq. (4), the standard difference approximation is:

$$\Delta F(y_i) = F(y_i) - F(y_{i-1}) = \frac{\sum_{i=0}^{i} n(y_i) - \sum_{i=0}^{i-1} n(y_i)}{\sum_{i=0}^{\infty} n(y_i)} = \frac{\left\{ n(y_i) + \sum_{i=0}^{i-1} n(y_i) \right\} - \sum_{i=0}^{i-1} n(y_i)}{\sum_{i=0}^{\infty} n(y_i)} = \frac{n(y_i)}{\sum_{i=0}^{\infty} n(y_i)}. \tag{6}$$

for $i = 1,2,3\ldots$. Thus, using Eq. (6), the probability density function becomes:

$$f(y_i) = \frac{n(y_i)}{\Delta y_i \sum_{i=0}^{\infty} n(y_i)} \tag{7}$$

Equation (7) satisfies the normalization property of Eq. (5) such that:

$$\int_0^{\infty} f(y)dy \approx \sum_{i=0}^{\infty} f(y_i)\Delta y_i = \frac{\sum_{i=0}^{\infty}\left[\left(\frac{n(y_i)}{\Delta y_i}\right)\Delta y_i\right]}{\sum_{i=0}^{\infty} n(y_i)} = 1. \tag{8}$$

The bin width Δy_i in Eq. (7) is defined for a given instrument gain. For the present TEPC unit, the high-gain region was 0 to 22 keV/μm, with a bin width of 0.092 keV/μm. This bin width provided an increased resolution for the high-count bins compared to the low-gain region which covers the remaining channels up to 1273 keV/μm with a bin width of 5 keV/μm.

The frequency-mean lineal energy $\bar{y}_F$ is the expectation value of y, as weighted by the frequency probability density, where from standard calculus theory:

$$\bar{y}_F = \frac{\int_0^{\infty} yf(y)dy}{\int_0^{\infty} f(y)dy} = \int_0^{\infty} yf(y)dy \approx \sum_{i=0}^{\infty} y_i f(y_i)\Delta y_i. \tag{9}$$

The second relation in Eq. (9) follows from the normalization of Eq. (5).

The dose-mean lineal energy $\bar{y}_D$ is the second moment, where from calculus theory:[32]

$$\bar{y}_D = \frac{\int_0^{\infty} y^2 f(y)dy}{\int_0^{\infty} yf(y)dy}. \tag{10}$$

As shown later, Eq. (10) is also the expectation value for the dose probability density. Substituting Eq. (9) into Eq. (10) yields:

$$\bar{y}_D = \frac{1}{\bar{y}_F}\int_0^{\infty} y^2 f(y)dy \approx \frac{1}{\bar{y}_F}\sum_{i=0}^{\infty} y_i^2 f(y_i)\Delta y_i. \tag{11}$$

The dose probability density $d(y)$ can be further defined as:

$$d(y) = \frac{1}{\bar{y}_F} y f(y) \tag{12}$$

so that Eq. (11) can be rewritten as:

$$\bar{y}_D = \int_0^\infty y d(y) dy. \tag{13}$$

Multiplying both sides of Eq. (12) by dy and integrating from 0 to ∞, it can be seen from Eq. (9) that the dose probability density also has the normalization property:

$$\int_0^\infty d(y) dy = 1. \tag{14}$$

Thus, from Eqs. (13) and (14), it follows that $\bar{y}_D$ is an expectation value of y weighted with the dose probability density.

For presentation purposes of the microdosimetric spectrum, the dose distribution is normally plotted as $y\ d(y)$ versus $\log y$. Here the ordinate in this semi-log representation is multiplied by y as a consequence of the logarithmic derivative

$$d(\ln y) = (\ln 10) d(\log y) = \frac{1}{y} dy. \tag{15}$$

Thus, using Eq. (15), the area deliminated by any two values of y is proportional to the fraction of *dose* delivered by events with lineal energies in this range, i.e.,

$$\int_{y_1}^{y_2} d(y) dy = \int_{y_1}^{y_2} [y d(y)] d \ln y = 2.303 \int_{y_1}^{y_2} [y d(y)] d \log y. \tag{16}$$

The TEPC is used to simulate a microscopic volume of tissue. This simulation is achieved by arranging the gas pressure in the low-density gas cavity of the TEPC so that

$$\rho_d d_d = \rho_t d_t \tag{17}$$

where ρ is the density and d is the diameter, and the subscripts d and t refer to the detector and tissue, respectively. The absorbed dose D in the detector and tissue site are equal:

$$D_d = \frac{\varepsilon_d}{m_d} = \frac{\varepsilon_d}{\rho_d V_d} = \frac{\varepsilon_t}{\rho_t V_t} = \frac{\varepsilon_t}{m_t} = D_t \tag{18}$$

where ε is the amount of energy deposited in either the detector (d) or site (t) of mass m. Note that by definition, the specific energy z is defined as:

$$z = \frac{\varepsilon}{m} \tag{19}$$

The volume V of the spherical detector cavity or tissue site is given by:

$$V_d = \frac{\pi}{6} d_d^3 \quad \text{and} \quad V_t = \frac{\pi}{6} d_t^3. \tag{20}$$

For the present TEPC unit, a detector diameter of 5 inches (i.e., $d_d = 1.27 \times 10^5$ μm) is used to simulate a spherical tissue site of diameter $d_t = 2$ μm. Using Eqs. (17), (18) and (20):

$$\varepsilon_t = \varepsilon_d \left(\frac{\rho_t}{\rho_d}\right)\left(\frac{V_t}{V_d}\right) = \varepsilon_d \left(\frac{\rho_t}{\rho_d}\right)\left(\frac{d_t^3}{d_d^3}\right) = \varepsilon_d \left(\frac{d_t^2}{d_d^2}\right). \tag{21}$$

The number of events in either the site or cavity is proportional to the amount of energy ε deposited in each. However, the energy *per event* is the same in the detector and simulated site due to their equivalence. Thus, Eq. (21) indicates that the number of events in the simulated site is less than the number of events in the detector by the ratio of their respective areas $(= d_t^2 / d_d^2)$.

For the dose calculation, it is important to relate the specific energy z (in Gy = J/kg) to the lineal energy y. The lineal energy y is the amount of energy ε deposited in the mean chord length $\overline{\ell}$:

$$y = \frac{\varepsilon}{\overline{\ell}} = \frac{z \cdot m}{\overline{\ell}} \tag{22}$$

for a site of mass m. The mean chord length can be calculated from Cauchy's theorem where for a convex site with a volume V and surface area S:[32]

$$\overline{\ell} = \frac{4V}{S}. \tag{23}$$

Thus, substituting Eq. (23) into (22) yields:

$$y = \frac{z \cdot m \cdot S}{4V} = \frac{z\rho S}{4} \Rightarrow z = \frac{4y}{\rho S} = \frac{y}{\pi r^2 \rho} \tag{24}$$

where a spherical tissue site of radius r (i.e., $S = 4\pi r^2$) has been assumed and ρ is the tissue density (which for microdosimetry is taken to be equal to 1 g/cm^3). Therefore, using the units with z in Gy (= J/kg), y in keV/μm and r in μm (with $\rho = 1$ g/cm^3), Eq. (24) becomes:

$$z\left(\frac{J}{kg}\right) = \frac{y\,(\cancel{keV}/\cancel{\mu m})}{\left(\frac{\pi}{4}\right) \times (2r)^2\,(\cancel{\mu m}^2) \times 1\,(\cancel{g}/\cancel{cm}^3)} \times \frac{1000\,\cancel{g}}{kg} \times \frac{1.602 \times 10^{-16} J}{\cancel{keV}} \times \frac{1\,\cancel{\mu m}^3}{(10^{-4})^3\,\cancel{cm}^3}$$

$$\Rightarrow z = \frac{0.204 y}{d_t^2} \tag{25a}$$

where d_t (= $2r$) is the diameter of the simulated tissue site.

The total absorbed dose in the ideal spherical gas cavity is equal to the average (frequency-mean) specific energy per event ($\overline{z}_F$) times the total number of events in the cavity, i.e., $\sum_{i=0}^{\infty} n(y_i)$. Equation (25a) also holds for the frequency means. For instance, the relationship, $f_1(z)dz = f(y)dy$, is valid for any volume where $f_1(z)$ is the single event distribution of z.[33] Therefore, multiplying this relation on both sides by z and integrating from 0 to ∞ yields the required result for the frequency means:

$$\bar{z}_F = \int_0^\infty z f_1(z)dz = \int_0^\infty z f(y)dy = \frac{0.204}{d_t^2}\int_0^\infty y f(y)dy = \frac{0.204}{d_t^2}\bar{y}_F \tag{25b}$$

where Eqs. (9) and (25a) have been used in the derivation. Thus, using Eqs. (9) and (25b), the total absorbed dose is given by:

$$D = \frac{0.204}{d_t^2}\bar{y}_F \sum_{i=0}^\infty n(y_i)\left(\frac{d_t^2}{d_d^2}\right) = \frac{0.204}{d_d^2}\left[\sum_{i=0}^\infty y_i f(y_i)\Delta y_i\right]\left[\sum_{i=0}^\infty n(y_i)\right]. \tag{26}$$

As discussed previously, in the derivation of the first relation, an area correction must be applied to the number of events in accordance with Eq. (21). Substituting Eq. (7) into (26) yields:

$$D = \frac{0.204}{d_d^2}\sum_{i=0}^\infty y_i n(y_i) \tag{27}$$

Similarly, the dose equivalent is given by

$$H = \frac{0.204}{d_d^2}\sum_{i=0}^\infty q(y_i) y_i n(y_i) \tag{28}$$

where $q(y)$ is the quality factor. Both Eqs. (27) and (28) have been proposed in Ref. 31. Using Eqs. (27) and (28), the average quality factor is further given by:

$$\bar{Q} = \frac{H}{D} = \frac{\sum_{i=0}^\infty q(y_i) y_i n(y_i)}{\sum_{i=0}^\infty y_i n(y_i)} = \frac{\left[\sum_{i=0}^\infty n(y_i)\right]\sum_{i=0}^\infty q(y_i) y_i f(y_i)\Delta y_i}{\left[\sum_{i=0}^\infty n(y_i)\right]\sum_{i=0}^\infty y_i f(y_i)\Delta y_i} \tag{29a}$$

$$= \frac{\int_0^\infty q(y) y f(y)dy}{\int_0^\infty y f(y)dy} = \frac{\int_0^\infty q(y) d(y)dy}{\int_0^\infty d(y)dy} = \int_0^\infty q(y)d(y)dy. \tag{29b}$$

In the derivation of Eq. (29a), Eq. (7) was used, while the second relation in Eq. (29b) results on use of Eqs. (12) and (14).

Finally, Eqs. (27) and (28) are only strictly applicable to an ideal detector. To account for non-spherical and field edge effects, the given detector must be calibrated so that a correction factor can be applied:

$$D_{real} = \xi D_{ideal} \text{ and } H_{real} = \xi H_{ideal} \tag{30}$$

where $\xi = 1.080$ for the present TEPC unit.

References

1. International Commission on Radiological Protection, "1990 Recommendations of the International Commission on Radiological Protection," ICRP Publications 60, Pergamon Press, Oxford (1991).

2. Health Protection Branch, "1997 Report on Occupational Radiation Exposures in Canada," Environmental Health Directorate, 97-EHD-213, (1997).

3. S. Vlahovich, private communication, Health Canada, April 1998.

4. Atomic Energy Control Board, "Proposed Amendments to the Atomic Energy Control Regulations for Reduced Radiation Dose Limits Based on the 1991 Recommendations of the International Commission on Radiological Protection," Consultative Document C-122, (1991).

5. P.R. Band, J.J. Spinelli, V.T.Y. Ng, J. Moody and R.P. Gallagher, "Mortality and Cancer Incidence in a Cohort of Commercial Airline Pilots," Aviation, Space and Environmental Medicine, Vol. 61, No. 4, 299-302 (1990).

6. P.R. Band, N.D. Le, R. Fang, M. Deschamps, A.J. Coldman, R.P. Gallagher and J. Moody, "Cohort Study of Air Canada Pilots: Mortality, Cancer Incidence and Leukemia Risk," American Journal of Epidemiology, Vol. 143, No. 2, 137-143 (1996).

7. D. Irvine, "A PMR Study of British Airways Pilot Mortality from 1966-1989," Proc. of the International Workshop on Cosmic Radiation, Electromagnetic Fields and Health Among Aircrews, Medical University of South Carolina, Charleston, South Carolina, February 5-7, 1998, p.37.

8. J.K. Grayson and T.J. Lyons, "Cancer Incidence in United States Air Force Aircrew, 1975-89," Aviation, Space and Environmental Medicine, Vol. 67, No. 2, 101-104 (1996).

9. B. Grajewski, E. Whelan, M. Waters and T. Bloom, "Estimating Radiation Dose for Epidemiological Studies," Proc. of the International Workshop on Cosmic Radiation, Electromagnetic Fields and Health Among Aircrews, Medical University of South Carolina, Charleston, South Carolina, February 5-7, 1998, pp. 40-42.

10. E. Pukka, A. Auvinen and G. Wahlberg," Incidence of Cancer Among Finnish Airline Cabin Attendants, 1967-92," BMJ Vol. 311, 649-652 (1995).

11. A. Auvinen, "Cancer Incidence in a Cohort of Finnish Airline Cabin Attendants," Proc. of the International Workshop on Cosmic Radiation, Electromagnetic Fields and Health Among Aircrews, Medical University of South Carolina, Charleston, South Carolina, February 5-7, 1998, p.35.

12. D. O'Sullivan, "Overview and Present Status of EC Research Programme," International Conference on Cosmic Radiation and Air Crew Exposure: Implementation of European Requirements in Civil Aviation, European Commission and Radiological Protection Institute of Ireland, Dublin, Ireland, July 1-3, 1998.

13. W. Friedberg, F.E. Duke, L. Snyder, K. Copeland, K. O'Brien, D.E. Parker, M.A. Shea and D.F. Smart, "CARI-LF," Civil Aeromedical Institute, Federal Aviation Administration, Oklahoma City, OK, private communication, May 1998.

14. P. Tume, "The Use and Characterisation of Bubble Detectors for the Assessment of the Occupational Exposure of Canadian Forces Pilots," Doctoral Thesis, Department of Chemistry and Chemical Engineering, Royal Military College of Canada, May (1996).

15. P. Tume, B.J. Lewis, L.G.I. Bennett and T. Cousins, "Characterisation of Neutron-Sensitive Bubble Detectors for Application in the Measurement of Jet Aircrew Exposure to Natural Background Radiation," Nucl. Instr. Meth. Phys. Res. A. Vol. 406, 153-168 (1998).

16. R. Noulty, private communication, Bubble Technology Industries, Inc., January 1996.

17. L.E. Moritz, "Measurement of Neutron Leakage Spectra at a 500-MeV Accelerator," Health Physics Vol. 56, No. 3, 287-296 (1989).

18. P. Tume, B.J. Lewis, L.G.I. Bennett, T. Cousins, T.A. Jones, B.E. Hoffarth, J.R. Brission, P. Goldhagen, A. Cavallo, W. Van Steveninck, M. Reginatto, P. Shebell, F. Hajnal, T.J. Jamieson and F.J. LeMay, "Assessment of the Cosmic Radiation Field at Jet Altitudes," Proceedings of the Radiation Protection and Shielding Topical Meeting, No. Falmouth, Massachusetts, April 21-25, 1996, pp. 68-75.

19. P. Goldhagen, private communication, Environmental Measurements Laboratory, March 1998.

20. S. Roesler, W. Heinrich and H. Schraube, "Calculation of Radiation Fields in the Atmosphere and Comparison to Experimental Data," Radiation Research Vol. 149, 87-97 (1998).

21. T.W. Armstrong, K.C. Chandler and J. Barish, "Calculations of Neutron Flux Spectra Induced in the Earth's Atmosphere by Galactic Cosmic rays," J. Geophysical Research Vol. 78, No. 16, 2715-2726 (1973).

22. W.N. Hess, H.W. Patterson, R. Wallace and E.L. Chupp, "Cosmic-Ray Neutron Energy Spectrum," Phys. Rev. Vol. 116, No. 2, 445-457 (1959).

23. W.N. Hess, E.H. Canfield and R.E. Lingenfelter, "Cosmic-Ray Neutron Demography," J. Geo. Phys. Res. Vol. 66, No. 3, 665-677 (1961).

24. B.R.L. Siebert and H. Schuhmacher, "Quality Factors, Ambient and Personal Dose Equivalent for Neutrons Based on the New ICRU Stopping Power Data for Protons and Alpha Particles," Radiat. Prot. Dosim. Vol. 58, No. 3, 177-183 (1995).

25. A. Sannikov and E.N. Savitskaya, "Ambient Dose Equivalent Conversion Factors for High Energy Neutrons Based on the ICRP-60 Recommendations," Radiat. Prot. Dosim. Vol. 70, Nos. 1-4, 383-386 (1997).

26. A. Ferrari, M. Pelliccioni and M. Pillon, "Fluence to Effective Dose Conversion Coefficients for Neutrons up to 10 TeV," Radiat. Prot. Dosim. Vol. 71, No. 3, 165-173 (1997).

27. P. Tume, L.G.I. Bennett, B.J. Lewis, H.K. Wieland, M.K. Reid, and T. Cousins, "Development of a Portable Micro-environmental Cell for the Testing of Neutron Bubble Detectors in a Simulated Jet-Aircraft Environment" 19th Annual Canadian Nuclear Society Conference, Toronto, Ontario, October 18-21 1998.

28. B.J. Lewis, R. Kosierb, T. Cousins, D.F. Hudson and G. Guéry, "Measurement of Neutron Radiation Exposure of Commercial Airline Pilots using Bubble Detectors," Nucl. Technol. Vol. 106, 373-383 (1994).

29. International Commission on Radiation Units and Measurements, "The Quality Factor in Radiation Protection," ICRU Publication 40, Bethesda, Maryland, U.S.A., April 1986.

30. A.J. Waker, "Principles of Experimental Microdosimetry," Radiat. Protect. Dosim. Vol. 61, No. 4, 297 (1995).

31. S. Gerdung, P. Pihlet, J.E. Grindborg, H. Roos, U.J. Schrewe and H. Schuhmacher, "Operation and Application of Tissue-Equivalent Proportional Counters", Radiat. Protect. Dosim. Vol. 61, No. 4, 381-404 (1995).

32. H.H. Rossi and M. Zaider, Microdosimetry and Its Applications, Springer-Verlag Berlin Heidelberg, New York (1996).

33. International Commission on Radiation Units and Measurements, "Microdosimetry," International Commission on Radiation Units and Measurements, ICRU Report 36, December 1983.

34. H. Schuhmacher and U.J. Schrewe, "Dose Equivalent Measurements on Board Civil Aircraft," Physikalisch Technische Bundesanstalt, PTB-Bericht, PTB-N-13, Braunschweig, March 1993.

35. P. Tume, B.J. Lewis, L.G.I Bennett, T. Cousins, T.A. Jones, B.E. Hoffarth and J.R. Brisson, "Canadian Aircrew Radiation Environment Study," Royal Military College of Canada, Report to Air Transport Association of Canada, March 1998.

36. M. Bagshaw, "Measurements," Proc. of the International Workshop on Cosmic Radiation, Electromagnetic Fields and Health Among Aircrews, Medical University of South Carolina, Charleston, South Carolina, February 5-7, 1998, pp. 8-9.

37. Commission of the European Communities, "Radiation Protection: Recommendations for the Implementation of Title VI of the European Basic Standards Directive (BSS) Concerning Significant Increase in Radiation Exposure due to Natural Radiation," Report of EURADOS Article 13 Working Group, December 1996.